The current issue and full text archive of this journal is available at
www.emeraldinsight.com/0961-5539.htm



# Mixed convection flow of a micropolar fluid near a non-orthogonal stagnation-point on a stretching vertical sheet

Y.Y. Lok
*Faculty of Manufacturing Engineering, Universiti Teknikal Malaysia Melaka, Ayer Keroh, Melaka, Malaysia*
I. Pop
*Faculty of Mathematics, University of Cluj, Cluj, Romania*
D.B. Ingham
*Centre for Computational Fluid Dynamics, University of Leeds, Leeds, UK, and*
N. Amin
*Department of Mathematics, Faculty of Science, Universiti Teknologi Malaysia, Skudai, Johor, Malaysia*

Received 18 July 2007
Revised 31 January 2008
Accepted 19 March 2008

## Abstract

**Purpose** – The purpose of this paper is to study theoretically the steady two-dimensional mixed convection flow of a micropolar fluid impinging obliquely on a stretching vertical sheet. The flow consists of a stagnation-point flow and a uniform shear flow parallel to the surface of the sheet. The sheet is stretching with a velocity proportional to the distance from the stagnation point while the surface temperature is assumed to vary linearly. The paper attempts also to show that a similarity solution of this problem can be obtained.

**Design/methodology/approach** – Using a similarity transformation, the basic partial differential equations are first reduced to ordinary differential equations which are then solved numerically using the Keller box method for some values of the governing parameters. Both assisting and opposing flows are considered. The results are also obtained for both strong and weak concentration cases.

**Findings** – These results provide information about the effect of $a/c$ (ratio of the stagnation point velocity and the stretching velocity), $\sigma$ (shear flow parameter) and $K$ (material parameter) on the flow and heat transfer characteristics in mixed convection flow near a non-orthogonal stagnation-point on a vertical stretching surface. The results show that the shear stress increases as $K$ increases, while the heat flux from the surface of the sheet decreases with an increase in $K$.

**Research limitations/implications** – The results in this paper are valid only in the small region around the stagnation-point on the vertical sheet. It is found that for smaller Prandtl number, there are difficulties in the numerical computation due to the occurrence of reversed flow for opposing flow. An extension of this work could be performed for the unsteady case.

**Originality/value** – The present results are original and new for the micropolar fluids. They are important in many practical applications in manufacturing processes in industry.

**Keywords** Flow, Convection, Fluid dynamics, Fluids

**Paper type** Research paper

The first author (Y.Y. Lok) would like to acknowledge the financial support received from the EU Marie Curie Training Site Grant and the host, the Centre for Computational Fluid Dynamics, University of Leeds, UK. The second and third authors (I. Pop and D.B. Ingham) wish to thank the Royal Society for partial financial support. The authors also thank the reviewers for their valuable comments and suggestions.

International Journal of Numerical Methods for Heat & Fluid Flow
Vol. 19 Nos. 3/4, 2009
pp. 459-483

0961-5539
DOI 10.1108/09615530910938380

## Nomenclature

| | |
|---|---|
| $a, b, c$ | constants |
| $A$ | constant in Equation (30) |
| $g$ | magnitude of the acceleration due to gravity |
| $Gr_x$ | local Grashof number |
| $j$ | microinertia density |
| $k$ | thermal conductivity |
| $K$ | material parameter |
| $\ell$ | characteristic length of the sheet |
| $n$ | ratio of the microrotation vector component and the fluid skin friction at the wall |
| $\overline{N}$ | component of the microrotation vector normal to $\overline{x}$–$\overline{y}$ plane |
| $N$ | non-dimensional component of the microrotation vector normal to $x - y$ plane |
| $\overline{p}$ | pressure |
| $p$ | non-dimensional pressure |
| Pr | Prandtl number |
| $\overline{q}_w$ | heat flux from the surface of the sheet |
| $q_w$ | non-dimensional heat flux from the surface of the sheet |
| $R$ | ratio of the slope of the dividing streamline near the wall to the slope far from the wall |
| $\mathrm{Re}_x$ | local Reynolds number |
| $\overline{T}$ | fluid temperature |
| $T$ | non-dimensional fluid temperature |
| $T_0$ | characteristic temperature |
| $\overline{u}, \overline{v}$ | velocity components along $\bar{x}$ and $\bar{y}$ axes |
| $u, v$ | non-dimensional velocity components along $x$ and $y$ axes |
| $\overline{x}, \overline{y}$ | Cartesian coordinates along the plate and normal to it, respectively |
| $x, y$ | non-dimensional Cartesian coordinates along the wall and normal to it, respectively |

*Greek symbols*

| | |
|---|---|
| $\alpha$ | thermal diffusivity |
| $\beta$ | thermal expansion coefficient |
| $\sigma$ | shear flow parameter |
| $\gamma$ | spin gradient viscosity |
| $\kappa$ | vortex viscosity |
| $\lambda$ | mixed convection parameter |
| $\mu$ | dynamic viscosity |
| $\upsilon$ | kinematic viscosity |
| $\rho$ | density |
| $\overline{\tau}_w$ | skin friction or shear stress from the surface of the sheet |
| $\tau_w$ | non-dimensional skin friction or shear stress from the surface of the sheet |
| $\psi$ | non-dimensional stream function at the plate |

*Subscripts*

| | |
|---|---|
| $w$ | wall condition |
| $\infty$ | far field condition |

## Introduction

The two-dimensional orthogonal or oblique stagnation-point flows of a viscous fluid impinging on a flat wall are very interesting problems in the history of fluid mechanics. These flows appear in virtually all flow fields of engineering and scientific interest. Hiemenz (1911) derived an exact solution of the Navier-Stokes equations, which describes the steady flow directed perpendicular (orthogonal) to an infinite flat plate. Stuart (1959), Tamada (1979), Dorrepaal (1986) and Labropulu *et al.* (1996) have extended the classical steady Hiemenz problem to oblique stagnation-point flow, while

Wang (1985) and Takemitsu and Matunobu (1979) presented exact solutions of the unsteady oblique stagnation-point flow. Dorrepaal *et al.* (1992) investigated the behaviour of a steady visco-elastic fluid impinging on a flat rigid wall at an arbitrary angle of incidence and found that the ratio of the two slopes depends upon the elastic effects of the fluid but it is independent of the angle of incidence of the streamline. Finally, we mention that Tilley and Weidman (1998) have studied the steady oblique two-fluid stagnation-point flow.

Great interest in micropolar fluids, which exhibit the microrotational effects and microrotational inertia, began very soon after the pioneering studies by Eringen (1966, 1972). Hoyt and Fabula (1964) have shown experimentally that fluids which cannot be characterized by Newtonian relationships, namely fluids containing minute polymeric additives indicate considerable reduction of the skin friction near a rigid body (about 25-30 per cent), and it can be well explained by the theory of micropolar fluids. Eringen's micropolar model includes the classical Navier-Stokes equations as a special case, but can cover, both in theory and applications, many more phenomena than the classical model. Examples of industrially relevant flows that can be studied using the micropolar theory include the flow of low concentration suspensions, liquid crystals, animal blood, colloidal fluids, lubrication, turbulent shear flow, etc. The micropolar fluid theory, introduced by Eringen (1966) was developed with the idea of explaining the behaviour of such fluids, giving rise to concepts such as microstress averages, inertial spin, stress and body moments; the microelements not only possess translation motion but can also undergo rotational motion. The interaction of the macro-velocity field and the microrotation field is described through new material constants in addition to those for a classical Newtonian fluid. Since the publication of Eringen's micropolar fluid theory, many authors have investigated various flow and heat transfer problems. Extensive reviews of the theory and applications can be found in the reviews articles by Ariman *et al.* (1973, 1974) and the recent books by Łukaszewicz (1999) and Eringen (2001).

Here we analyse the steady two-dimensional stagnation-point flow of a micropolar fluid impinging on a continuously moving vertical sheet obliquely. In particular, we investigate the behaviour of the micropolar fluid near the vertical sheet for various values of the governing non-dimensional parameters. The objective of this paper is also to show that a similarity solution of the governing equations can be obtained for the mixed convection flow over a continuous moving vertical sheet in a micropolar fluid. From a mathematical point of view, this problem is of interest because it represents one of the relatively few instances in fluid mechanics where exact similarity solutions of the full governing partial differential equations can be obtained. It is important to mention that the problem of heat transfer in the boundary layer over a continuously moving surface has many practical applications in manufacturing processes in industry. In these processes, the common method employed is to draw a hot material through a slot (or an orifice) in sheet (or fibre) manufacturing. During the process of drawing, the sheets are sometimes stretched and the rate of cooling has a great effect on the properties of the desired material structure. By drawing them in a micropolar fluid the rate of cooling may be controlled (Lakshmisha *et al.* (1988), Bhargava *et al.* (2003)). The thermal processing of sheet-like materials is a necessary operation in the production of paper, linoleum, polymeric sheets, roofing shingles and insulating materials (see Sparrow and Abraham (2005)). The tangential velocity imparted by the sheet induces motion in the surrounding fluid, which alters the convection cooling of the sheet. Due to the much higher viscosity of the extrusate, one can assume the fluid is affected by the sheet but not vice versa. Experiments show that the velocity of the boundary is approximately proportional to the

distance from the orifice (see Vleggaar (1977)). Other applications include hot rolling, glass-fibre, paper production, metal and polymer extrusion, etc. (see Magyari and Keller, 1999). The flow and heat transfer of a viscous and incompressible fluid (Newtonian fluid) over a continuous moving vertical surface has been studied by several authors such as Daskalakis (1993), Ali and Al-Yousef (1998), Chen (1998, 2000), Partha *et al.* (2005) and very recently by Ishak *et al.* (2006a, b).

## Basic equations

Consider the steady two-dimensional flow of a micropolar fluid near a non-orthogonal stagnation-point on a vertical stretching flat plate coinciding with the plane $\overline{y} = 0$ as shown in Figure 1. Cartesian coordinates $(\overline{x}, \overline{y})$ are taken such that the $\overline{x}$-axis is measured along the sheet oriented in the upward direction and the $\overline{y}$-axis is normal to it. It is assumed that the far-flow (inviscid) impinges on the stretching surface consists of a stagnation point flow and a uniform shear flow parallel to the wall with the velocity $\overline{V}_e(\overline{u}_e, \overline{v}_e)$. It is also assumed that the flat plate is stretched with a velocity $\overline{u}_w(\overline{x})$ and that the temperature of the plate is $\overline{T}_w(\overline{x})$, while the ambient fluid is at a constant temperature $T_\infty$, where $\overline{T}_w(x) > T_\infty$ (heated plate) or $\overline{T}_w(x) < T_\infty$ (cooled plate), respectively. Further, both $\overline{u}_w(\overline{x})$ and $\overline{T}_w(\overline{x})$ are assumed to vary linearly with $\overline{x}$. The assisting flow occurs if the upper half of the sheet is heated while the lower half of the sheet is cooled. In this case, the flow near the heated sheet tends to move upward and the flow near the cooled sheet tends to move download, therefore this behaviour acts to assist the flow field. The opposing flow occurs if the upper part of the sheet is cooled while the lower part of the sheet is heated, see Figure 1. Under these assumptions, together with the Boussinesq approximations, the steady two-dimensional flow of a micropolar fluid is described by the following equations:

$$\frac{\partial \overline{u}}{\partial \overline{x}} + \frac{\partial \overline{v}}{\partial \overline{y}} = 0 \tag{1}$$

$$\overline{u}\ \frac{\partial \overline{u}}{\partial \overline{x}} + \overline{v}\ \frac{\partial \overline{u}}{\partial \overline{y}} = -\frac{1}{\rho}\frac{\partial \overline{p}}{\partial \overline{x}} + \left(\frac{\mu + \kappa}{\rho}\right)\overline{\nabla}^2 \overline{u} + \frac{\kappa}{\rho}\frac{\partial \overline{N}}{\partial \overline{y}} + g\,\beta\,(\overline{T} - T_\infty) \tag{2}$$

$$\overline{u}\ \frac{\partial \overline{v}}{\partial \overline{x}} + \overline{v}\ \frac{\partial \overline{v}}{\partial \overline{y}} = -\frac{1}{\rho}\frac{\partial \overline{p}}{\partial \overline{y}} + \left(\frac{\mu + \kappa}{\rho}\right)\overline{\nabla}^2 \overline{v} - \frac{\kappa}{\rho}\frac{\partial \overline{N}}{\partial \overline{x}} \tag{3}$$

$$\rho j\left(\overline{u}\ \frac{\partial \overline{N}}{\partial \overline{x}} + \overline{v}\ \frac{\partial \overline{N}}{\partial \overline{y}}\right) = \gamma\,\overline{\nabla}^2 \overline{N} - \kappa\left(2\overline{N} + \frac{\partial \overline{u}}{\partial \overline{y}} - \frac{\partial \overline{v}}{\partial \overline{x}}\right) \tag{4}$$

$$\overline{u}\ \frac{\partial \overline{T}}{\partial \overline{x}} + \overline{v}\ \frac{\partial \overline{T}}{\partial \overline{y}} = \alpha \overline{\nabla}^2 \overline{T} \tag{5}$$

which have to be solved subject to the boundary conditions

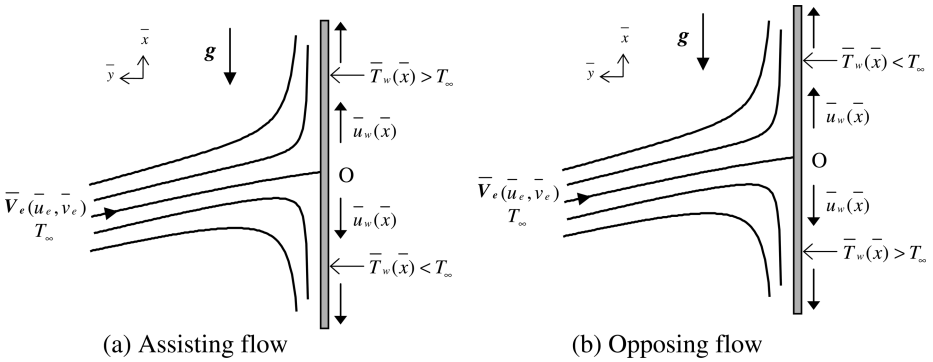


**Figure 1.**
Physical model and coordinate system

$$\begin{aligned} &\bar{v} = 0, \quad \bar{u} = \bar{u}_w(\bar{x}) = c\,\bar{x}, \quad \overline{T} = \overline{T}_w(\bar{x}) = T_\infty + T_0\,(\bar{x}/\ell), \\ &\overline{N} = -n\left(\frac{\partial \bar{u}}{\partial \bar{y}} - \frac{\partial \bar{v}}{\partial \bar{x}}\right) \quad \text{at} \quad \bar{y} = 0 \qquad \bar{u} = \bar{u}_e = a\,\bar{x} + b\,\bar{y}, \\ &\bar{v} = \bar{v}_e = -a\,\bar{y}, \quad \overline{T} = T_\infty, \quad \overline{N} = \text{constant} = c_1 \quad \text{as} \quad \bar{y} \to \infty \end{aligned} \tag{6}$$

where $\bar{u}$ and $\bar{v}$ are the velocity components along the $\bar{x}$ and $\bar{y}$ axes, respectively, $\overline{T}$ is the fluid temperature, $T_0$ is the characteristic temperature, $\bar{p}$ is the pressure, $\overline{N}$ is the component of the microrotation vector normal to the $\bar{x} - \bar{y}$ plane, $\rho$ is the density, $g$ is the magnitude of the acceleration due to gravity, $\ell$ is the characteristic length of the sheet, $\alpha$ is the thermal diffusivity, $\beta$ is the thermal expansion coefficient, $\mu$ is the dynamic viscosity, $\kappa$ is the vortex viscosity, $\gamma$ is the spin-gradient viscosity, $j$ is the microinertia density and $\overline{\nabla}^2$ is the Laplacian in Cartesian coordinates ($\bar{x}$, $\bar{y}$). It is assumed that all the physical quantities $\alpha$, $\beta$, $\rho$, $\mu$, $\kappa$, $\gamma$ and $j$ are constants. We notice from Equation (4) when $\bar{y} \to \infty$ that $b = c_1 = 0$ for the orthogonal stagnation point and $c_1 = -b/2$ ($b \neq 0$) for the non-orthogonal stagnation point flow, respectively. Further, $n$ is a constant such that $0 \leq n \leq 1$. It should be mentioned that the case $n = 0$, called strong concentration by Guram and Smith (1980), indicates that $\overline{N} = 0$ near the wall. This represents that the concentrated particle flows in which the microelements close to the wall surface are unable to rotate (Jena and Mathur, 1981). The case $n = 1/2$ indicates the vanishing of the anti-symmetrical part of the stress tensor and denotes weak concentration (Ahmadi, 1976). The case $n = 1$, as suggested by Peddieson (1972), is used for the modelling of turbulent boundary layer flows. The relation

$$\gamma = (\mu + \kappa/2), \; j = \mu\,(1 + K/2)\,j \tag{7}$$

where $K = \kappa/\mu$ is called the material or micropolar parameter and it is invoked to allow the field equations of the micropolar fluids to predict the correct behaviour in the limiting case when the microstructure effects become negligible and the total spin $\overline{N}$ reduces to the angular flow velocity or flow vorticity. This relation was established by Ahmadi (1976) and Kline (1977), and it has been used by many researchers, such as, for example, Gorla (1988), Rees and Bassom (1996), Rees and Pop (1998) and Nazar *et al.* (2003).

We introduce now the following non-dimensional variables

$$x = \overline{x}/\ell, \quad y = \overline{y}/\ell, \quad u = \overline{u}/(c\,\ell), \quad v = \overline{v}/(c\,\ell), \quad N = \overline{N}/c$$
$$T = (\overline{T} - T_\infty)/T_0, \quad p = \overline{p}/(\rho\, c^2\, \ell^2) \tag{8}$$

and we take $j = \upsilon/c = \ell^2$ where $j$ defines the length scale, $\ell$, see Rees and Bassom (1996), and $\upsilon$ is the kinematic viscosity. Substituting expressions (7) and (8) into Equations (1)-(5), they become in non-dimensional form

$$\frac{\partial u}{\partial x} + \frac{\partial v}{\partial y} = 0 \tag{9}$$

$$u\ \frac{\partial u}{\partial x} + v\ \frac{\partial u}{\partial y} = -\ \frac{\partial p}{\partial x} + (1+K)\,\nabla^2 u + K\ \frac{\partial N}{\partial y} + \lambda\ T \tag{10}$$

$$u\ \frac{\partial v}{\partial x} + v\ \frac{\partial v}{\partial y} = -\ \frac{\partial p}{\partial y} + (1+K)\,\nabla^2 v - K\ \frac{\partial N}{\partial x} \tag{11}$$

$$u\ \frac{\partial N}{\partial x} + v\ \frac{\partial N}{\partial y} = \left(1 + \frac{K}{2}\right)\nabla^2 N - K\left(2N + \frac{\partial u}{\partial y} - \frac{\partial v}{\partial x}\right) \tag{12}$$

$$u\ \frac{\partial\, T}{\partial\, x} + v\ \frac{\partial\, T}{\partial\, y} = \frac{1}{\mathrm{Pr}}\ \nabla^2 T \tag{13}$$

which have to be solved subject to the boundary conditions (6) which become

$$u = x, \quad v = 0, \quad T = x, \quad N = -n\left(\frac{\partial\, u}{\partial\, y} - \frac{\partial\, v}{\partial\, x}\right) \quad \text{at} \quad y = 0$$
$$u = \frac{a}{c}\,x\ +\ \sigma y, \quad v = -\frac{a}{c}\,y, \quad T = 0, \quad N = c_2 \quad \text{as} \quad y \to \infty \tag{14}$$

where $\sigma = c_2 = 0$ for the orthogonal stagnation-point flow and $c_2 = -\sigma/2$ ($\sigma \neq 0$) for the non-orthogonal stagnation point flow, respectively. Here, $\sigma = b/c$ is the shear flow parameter, $\mathrm{Pr} = \upsilon/\alpha$ is the Prandtl number and $\lambda$ is the constant mixed convection parameter which is defined as

$$\lambda = \frac{Gr_x}{\mathrm{Re}_x^2} \tag{15}$$

where $Gr_x = g\,\beta(\,\overline{T}_w - T_\infty)\overline{x}^3/\upsilon^2$ is the local Grashof number and $\mathrm{Re}_x = \overline{u}_w(\overline{x})\overline{x}/\upsilon$ is the local Reynolds number. In this problem, $\lambda > 0$ corresponding to assisting flow, $\lambda < 0$ corresponding to opposing flow and $\lambda = 0$ corresponds to the forced convection flow. It should be mentioned that the boundary condition (14) for non-orthogonal stagnation-point flow, i.e. $N = -(1/2)\sigma$ is obtained by solving Equation (12) when $y \to \infty$.

Further, we introduce the stream function $\psi$ defined as

$$u = \frac{\partial \psi}{\partial y}, \quad v = -\ \frac{\partial \psi}{\partial x} \tag{16}$$

and eliminating the pressure $p$ from Equations (10) and (11), we obtain

$$\frac{\partial\psi}{\partial x}\frac{\partial}{\partial y}(\nabla^2\psi) - \frac{\partial\psi}{\partial y}\frac{\partial}{\partial x}(\nabla^2\psi) + (1+K)\,\nabla^4\psi + K\,\nabla^2 N + \lambda\,\frac{\partial T}{\partial y} = 0 \tag{17}$$

$$\frac{\partial\psi}{\partial y}\frac{\partial N}{\partial x} - \frac{\partial\psi}{\partial x}\frac{\partial N}{\partial y} = \left(1+\frac{K}{2}\right)\nabla^2 N - K\,(2N + \nabla^2\psi) \tag{18}$$

$$\frac{\partial\psi}{\partial y}\frac{\partial T}{\partial x} - \frac{\partial\psi}{\partial x}\frac{\partial T}{\partial y} = \frac{1}{\mathrm{Pr}}\nabla^2 T \tag{19}$$

subject to the boundary conditions

$$\begin{aligned} &\psi = 0, \quad \frac{\partial\psi}{\partial y} = x, \quad T = x, \quad N = -n\,\nabla^2\psi \quad \text{at} \quad y = 0 \\ &\psi = \frac{a}{c}\,xy + \frac{1}{2}\sigma y^2, \quad T = 0, \quad N = c_2 \quad \text{as} \quad y \to \infty \end{aligned} \tag{20}$$

where the $c_2$ is that defined above.

The physical quantities of interest are the skin friction or wall shear stress and the heat flux from the surface of the sheet which are defined as

$$\overline{\tau}_w = \left[(\mu+\kappa)\left(\frac{\partial\overline{u}}{\partial\overline{y}} + \frac{\partial\overline{v}}{\partial\overline{x}}\right) + \kappa\,\overline{N}\right]_{\overline{y}=0}, \quad \overline{q}_w = -k\left(\frac{\partial\overline{T}}{\partial\overline{y}}\right)_{\overline{y}=0} \tag{21}$$

where $k$ is the thermal conductivity. Using the expressions (8), (16) and (20), the non-dimensional skin friction or shear stress $\tau_w$ and the heat flux from the surface of the sheet $q_w$ can be written as

$$\tau_w = \left[(1+K)\left(\frac{\partial^2\psi}{\partial y^2} - \frac{\partial^2\psi}{\partial x^2}\right) + KN\right]_{y=0}, \qquad q_w = -\left(\frac{\partial T}{\partial y}\right)_{y=0} \tag{22}$$

where $\tau_w = \overline{\tau}_w/(\mu c)$ and $q_w = \overline{q}_w\ell/(kT_0)$.

**Orthogonal stagnation-point flow**

In this case $\sigma = c_2 = 0$ and the boundary conditions (20) become

$$\begin{aligned} &\psi = 0, \quad \frac{\partial\psi}{\partial y} = x, \quad T = x, \quad N = -n\,\nabla^2\psi \quad \text{on} \quad y = 0 \\ &\psi \sim \frac{a}{c}\,xy, \quad T \to 0, \quad N \to 0 \quad \text{as} \quad y \to \infty \end{aligned} \tag{23}$$

The boundary conditions (23) indicate the following similarity solution

$$\psi(x,y) = x f(y), \quad T(x,y) = x\,\Theta(y), \quad N(x,y) = x\,h(y) \tag{24}$$

Substituting (24) into Equations (17)-(19), we obtain, after one integration of Equation (17), the following ordinary differential equations

$$(1+K)f''' + ff'' + \left(\frac{a}{c}\right)^2 - f'^2 + K\,h' + \lambda\,\Theta = 0 \tag{25}$$

$$\left(1+\frac{K}{2}\right)h'' + f\,h' - f'\,h - K\,(2\,h + f'') = 0 \tag{26}$$

$$\frac{1}{\Pr}\,\Theta'' + f\,\Theta' - f'\,\Theta = 0 \tag{27}$$

subject to the boundary conditions (23) which become

$$\begin{aligned} f(0) = 0, \quad f'(0) = 1, \quad \Theta(0) = 1, \quad h(0) = -\,n f''(0) \\ f'(\infty) = \frac{a}{c}, \quad \Theta(\infty) = 0, \quad h(\infty) = 0 \end{aligned} \tag{28}$$

where primes denote differentiation with respect to $y$. It is worth mention that for $K = 0$ (Newtonian fluid), Equations (25)-(27) reduce to those considered by Ishak *et al.* (2006a).

In this case, the skin friction and the heat flux from the surface of the sheet (22) become

$$\tau_w = [1 + (1-n)K]\,x f''(0), \quad q_w = -\,x\,\Theta'(0) \tag{29}$$

if the boundary conditions (28) are used.

We notice that the function $f(y)$ behaves as

$$f(y) \sim \frac{a}{c}\,y + A \tag{30}$$

when $y \to \infty$, where $A$ is a constant of integration. The values of $A$ for $\Pr = 1$ and various values of the parameters $K$ and $a/c$ when $n = 0$ (strong concentration) and $n = 1/2$ (weak concentration) are given in Table I for assisting and opposing flows. It is found that when $K$ is fixed, the value of $A$ decreases as $a/c$ increases for both assisting and opposing flows. For fixed $a/c$, the values of $A$ increases as $K$ increases. It is also noticed that when $K = 1$ and 3, the values of $A$ for $n = 0$ are greater than the case when $n = 1/2$.

**Table I.**
Values of $A$ for various values of $a/c$ and $K$ when $\Pr = 1$, $n = 0$ (strong concentration) and $n = 1/2$ (weak concentration)

| | $\lambda = 1$ (assisting flow) | | | | | $\lambda = -1$ (opposing flow) | | | | |
|---|---|---|---|---|---|---|---|---|---|---|
| | $n = 0$ and $1/2$ | $n = 0$ | | $n = 1/2$ | | $n = 0$ and $1/2$ | $n = 0$ | | $n = 1/2$ | |
| $a/c$ | $K = 0$ | $K = 1$ | $K = 3$ | $K = 1$ | $K = 3$ | $K = 0$ | $K = 1$ | $K = 3$ | $K = 1$ | $K = 3$ |
| 0.1 | 1.0384 | 1.2299 | 1.5012 | 1.1886 | 1.4227 | – | 0.7431 | 1.2357 | – | 0.9957 |
| 0.5 | 0.4753 | 0.5634 | 0.6829 | 0.5421 | 0.6402 | 0.1223 | 0.3089 | 0.4996 | 0.2220 | 0.3764 |
| 1.0 | 0.0888 | 0.0737 | 0.0591 | 0.0874 | 0.0797 | −0.1020 | −0.0812 | −0.0631 | −0.0978 | −0.0867 |
| 1.5 | −0.1692 | −0.2672 | −0.3891 | −0.2208 | −0.3063 | −0.2950 | −0.3742 | −0.4773 | −0.3458 | −0.4230 |
| 2.0 | −0.3659 | −0.5331 | −0.7461 | −0.4577 | −0.6059 | −0.4571 | −0.6127 | −0.8135 | −0.5495 | −0.6934 |

**Oblique stagnation-point flow**

The boundary conditions (20) are now given by

$$\psi = 0, \quad \frac{\partial \psi}{\partial y} = x, \quad T = x, \quad N = -n\,\nabla^2\psi \quad \text{at} \quad y = 0$$
$$\psi = \frac{a}{c}\,x\,y + \frac{1}{2}\sigma y^2, \quad T = 0, \quad N = -\frac{1}{2}\,\sigma \quad \text{as} \quad y \to \infty \tag{31}$$

where $c_2 = -\sigma/2\ (\neq 0)$. These boundary conditions suggest that Equations (17)-(19) have the solution of the form

$$\psi(x,y) = xF(y) + G(y), \quad T(x,y) = x\,\theta(y)\ +\ \phi(y), \quad N(x,y) = xH(y) + S(y) \tag{32}$$

Substituting (32) into Equations (17)-(19) results in, after one integration of the equation for $F(y)$ and $G(y)$, the following ordinary differential equations

$$(1+K)\,F''' + F\,F'' + \left(\frac{a}{c}\right)^2 - F'^2 + K\,H' + \lambda\,\theta = 0 \tag{33}$$

$$(1+K)\,G''' + F\,G'' - F'\,G' + K\,S' + \lambda\,\phi - \sigma A = 0 \tag{34}$$

$$\left(1+\frac{K}{2}\right)H'' + F\,H' - F'H - K\,(2H + F'') = 0 \tag{35}$$

$$\left(1+\frac{K}{2}\right)S'' + F\,S' - G'\,H - K\,(2\,S + G'') = 0 \tag{36}$$

$$\frac{1}{\mathrm{Pr}}\,\theta'' + F\,\theta' - F'\,\theta = 0 \tag{37}$$

$$\frac{1}{\mathrm{Pr}}\,\phi'' + F\,\phi' - G'\,\theta = 0 \tag{38}$$

subject to

$$F(0) = 0, \ \ F'(0) = 1, \ \ \theta(0) = 1, \ \ H(0) = -nF''(0), \ \ F'(\infty) = \frac{a}{c}, \ \ \theta(\infty) = 0,$$
$$H(\infty) = 0, \tag{39a}$$
$$\phi(0) = 0, \ \ G(0) = G'(0) = 0, \ \ S(0) = -nG''(0), \ \ G''(\infty) = \sigma, \ \ \phi(\infty) = 0,$$
$$S(\infty) = -\frac{1}{2}\sigma. \tag{39b}$$

It is noticed that the differential Equations (33), (35) and (37) are identical with those of Equations (25)-(27) so that $F(y) \sim (a/c)\,y + A$ as $y \to \infty$.

Employing (32) in (22), the non-dimensional shear stress $\tau_w$ and the heat flux $q_w$ can be written as

$$\tau_w = [1 + (1-n)K]\ [xF''(0) + G''(0)]\,, \quad q_w = -[x\,\theta'(0)\ +\ \phi'(0)] \tag{40}$$

if the boundary conditions (39) are used. Values of $F''(0)$, $G''(0)$, $-\theta'(0)$ and $-\phi'(0)$ can be calculated for different values of Pr, $K$, $\Lambda$, $\lambda$, $n$ and $\sigma$. Thus, the streamlines $\psi$ can

be calculated using (32). In particular, the streamlines $\psi = 0$ meets the wall at $x = x_0$ (point of zero skin friction, $\tau_w = 0$) where, from (40), $x_0$ is given by

$$x_0 = -\frac{G''(0)}{F''(0)} \tag{41}$$

Introducing the new variables

$$G'(y) = \sigma M(y), \quad S(y) = \sigma P(y), \quad \phi(y) = \sigma Q(y) \tag{42}$$

Equations (34), (36) and (38) become

$$(1+K)M'' + FM' - F'M + KP' + \lambda T - A = 0 \tag{43}$$

$$\left(1+\frac{K}{2}\right)P'' + FP' - MH - K(2P + M') = 0 \tag{44}$$

$$\frac{1}{\mathrm{Pr}}Q'' + FQ' - M\theta = 0 \tag{45}$$

with the boundary conditions (39b) which become

$$\begin{aligned} &M(0) = 0, \quad P(0) = -nM'(0), \quad Q(0) = 0, \quad M'(\infty) = 1, \\ &Q(\infty) = 0, \quad P(\infty) = -\frac{1}{2}. \end{aligned} \tag{46}$$

where

$$G(y) = \sigma \int_0^\infty M(y)\, dy \tag{47}$$

The Maclaurin series for $F(y)$ and $G(y)$ near the wall $y \sim 0$ are given by

$$F(y) = y + \frac{1}{2}y^2F''(0) + \frac{1}{6}y^3F'''(0) + \text{h.o.t.} \tag{48}$$

$$G(y) = \frac{1}{2}y^2\sigma M'(0) + \frac{1}{6}y^3\sigma M''(0) + \text{h.o.t.} \tag{49}$$

Substituting Equations (42), (48) and (49) into Equation (32), we obtain the stream function $\psi(x,y)$ near the wall

$$\psi(x,y) = xy + \frac{1}{2}xy^2F''(0) + \frac{1}{6}xy^3F'''(0) + \frac{1}{2}y^2\sigma M'(0) + \frac{1}{6}y^3\sigma M''(0) + \text{h.o.t.} \tag{50}$$

which can be rewritten as

$$\psi(x,y) = y\left[x + \frac{1}{2}y\sigma M'(0) + \text{h.o.t.}\right] \tag{51}$$

Thus, near the wall, the dividing streamline $\psi = 0$ has the equation

$$x + \frac{1}{2} y\sigma M'(0) = 0 \tag{52}$$

and its slope $m_s$ near the wall is given by

$$m_s = -\frac{2}{\sigma\, M'(0)} \tag{53}$$

Letting $m_\infty$ to be the slope of the dividing streamline far from the wall, from boundary condition (31), we obtain

$$m_\infty = -\frac{2(a/c)}{\sigma} \tag{54}$$

and the ratio $R$ is found to be

$$R = \frac{m_s}{m_\infty} = \frac{1}{(a/c)\, M'(0)} \tag{55}$$

In Equation (55), it is noticed that the slope ratio is independent of shear flow parameter $\sigma$ of the dividing streamline at infinity. The same conclusions are reported by Dorrepaal (1986) and Labropulu *et al.* (1996) for Newtonian fluids ($K = 0$).

## Numerical method

The ordinary differential Equations (25)-(27), subject to the boundary conditions (28), as well as Equations (33)-(38), subject to the boundary conditions (39), have been solved numerically using the Keller box method for both orthogonal and oblique stagnation-point flows, respectively. In this approach, the differential equations are first reduced to a system of first-order ordinary differential equations, which are then expressed in finite-difference form using central differences. This system of equations is linearized using Newton's method before putting them in matrix-vector form. The resulting linear system of equations is solved along with their boundary conditions by the block-tridiagonal-elimination method. The details of this method are very well described in the books by Cebeci and Bradshaw (1984) and Cebeci (2002). In this paper, a step size of $\Delta y = 0.005$ is used, $y_\infty = 20$ and the convergence criterion is $5 \times 10^{-7}$. However, for $\mathrm{Pr} = 100$, we have taken $\Delta y = 0.001$ so that the results are mesh independent.

## Results and discussion

For comparison purposes, the values of $-\Theta'(0)$ for various values of $K$ and Pr when $a/c = 0$ (potential flow is absent), $n = 0$ (strong concentration) and $\sigma = 0$ (orthogonal stagnation-point flow) are given in Table II. Both assisting and opposing flow cases are considered. Besides, the values of the non-dimensional skin friction or shear stress$\tau_w = xF''(0) + G''(0)$ at $x = 1$ for several values of $a/c$ and $\sigma$ when $K = 0$ (Newtonian fluid) and $\lambda = 0$ (forced convection) are shown in Table III for the oblique stagnation-point flow case. The results reported by Grubka and Bobba (1985) for orthogonal stagnation-point flow are included in Table II and those reported by Mahapatra *et al.* (2007) for obqliue stagnation-point flow are included in Table III. The results for $f''(0)$ are the same as those obtained by Ishak *et al.* (2006a) who use the

**Table II.**
Values of $-\Theta'(0)$ for various values of Prandtl number Pr, mixed convection parameter $\lambda$ and material parameter $K$ when $a/c = n = 0$ and $\sigma = 0$ (orthogonal flow)

| | $\lambda = -1$ (opposing flow) | | | $\lambda = 0$ | | | $\lambda = 1$ (assisting flow) | | | $\lambda = 10$ (assisting flow) | | |
|---|---|---|---|---|---|---|---|---|---|---|---|---|
| Pr | $K = 0$ | $K = 1$ | $K = 3$ | $K = 0$ | $K = 1$ | $K = 3$ | $K = 0$ | $K = 1$ | $K = 3$ | $K = 0$ | $K = 1$ | $K = 3$ |
| 0.7 | – | – | 0.8753 | 0.7937 | 0.8667 | 0.9197 | 0.8961 | 0.9223 | 0.9490 | 1.1724 | 1.1272 | 1.0910 |
| 1 | – | – | 1.0980 | 1.0000 (1.0000) | 1.0745 | 1.1275 | 1.0873 | 1.1203 | 1.1513 | 1.3716 | 1.3220 | 1.2849 |
| 3 | 1.8586 | 1.9706 | 2.0382 | 1.9237 (1.9237) | 1.9991 | 2.0521 | 1.9743 | 2.0248 | 2.0652 | 2.2442 | 2.1925 | 2.1633 |
| 7 | 3.0361 | 3.1302 | 3.1920 | 3.0723 | 3.1476 | 3.2007 | 3.1055 | 3.1644 | 3.2092 | 3.3318 | 3.2935 | 3.2797 |
| 10 | 3.6912 | 3.7816 | 3.8420 | 3.7207 (3.7207) | 3.7960 | 3.8492 | 3.7486 | 3.8101 | 3.8563 | 3.9524 | 3.9231 | 3.9167 |
| 100 | 12.2851 | 12.3648 | 12.4207 | 12.2941 (12.2941) | 12.3693 | 12.4229 | 12.3031 | 12.3738 | 12.4252 | 12.3821 | 12.4139 | 12.4454 |

**Note:** ( ) Results by Grubka and Bobba (1985)

| $a/c$ | $\sigma \to 0.1$ | 0.2 | 1.0 | 2.0 | 4.0 | 6.0 |
|---|---|---|---|---|---|---|
| 0.1 | −0.9430 (−0.9431) | −0.9167 (−0.9168) | −0.7060 (−0.7061) | −0.4426 (−0.4427) | 0.0842 0.0841) | 0.6109 (0.6108) |
| 0.3 | −0.7888 (−0.7888) | −0.7282 (−0.7282) | −0.2431 (−0.2432) | 0.3632 (0.3631) | 1.5757 (1.5757) | 2.7883 (2.7883) |
| 0.8 | −0.2059 (−0.2059) | −0.1125 (−0.1125) | 0.6353 ( 0.6353) | 1.5700 (1.5700) | 3.4395 (3.4395) | 5.3089 (5.3089) |
| 1.0 | 0.1000 (0.1000) | 0.2000 (0.2000) | 1.0000 (1.0000) | 2.0000 (2.0000) | 4.0000 (4.0000) | 6.0000 (6.0000) |
| 2.0 | 2.1341 (2.1342) | 2.2507 (2.2507) | 3.1829 (3.1829) | 4.3481 (4.3481) | 6.6787 (6.6786) | 9.0092 (9.0091) |
| 3.0 | 4.8532 (4.8531) | 4.9766 (4.9766) | 5.9644 (5.9644) | 7.1992 (7.1991) | 9.6687 (9.6685) | 12.1382 (12.1378) |
| 4.0 | 8.1287 (8.1285) | 8.2560 (8.2558) | 9.2745 (9.2742) | 10.5477 (10.5473) | 13.0940 (13.0934) | 15.6403 (15.6395) |

**Note:** ( ) Results by Mahapatra *et al.* (2007)

**Table III.**
Values of $\tau_w = xF''(0) + G''(0)$ for various values of $\sigma$ (non-orthogonal flow) and $a/c$ when $x = 1, K = 0$ (Newtonian fluid) and $\lambda = 0$ (forced convection)

same numerical method, and therefore they are not presented in Table II. For the results in Table III, it should be mentioned that due to the different notation/definition, we have to consider the shear flow parameter $\sigma = 2(b/c)^*$, where $(b/c)^*$ is the shear flow parameter defined in the paper by Mahapatra *et al.* (2007). It can be seen from Tables II and III that the present results show very good agreement with those obtained by Grubka and Bobba (1985) and Mahapatra *et al.* (2007). Therefore we are confident that all the present results are very accurate.

It is observed from Table II that increasing the material parameter $K$ results in an increase in the value of the heat transfer from the plate, $-\Theta'(0)$ for both assisting and opposing flow cases. This indicates that for the case when the potential flow is absent, the micropolar fluid enhances the heat trasnfer process when compared to the Newtonian fluid ($K = 0$). It is also seen that the value of $-\Theta'(0)$ increases when Pr increases. It is further observed from Table II that for the case of opposing flow ($\lambda < 0$), some of the results could not be obtained for small values of Pr. The same phenomenon is also reported in the paper by Ishak *et al.* (2006a) for Newtonian fluid. This is supported by Figure 2 which shows the velocity and microrotation profiles, say for $\lambda = -1$, $\mathrm{Pr} = 1$ and $K = 1$, by assuming the boundary layer thickness is $y_\infty = 5$, 6 and 6.6. In this case, it is noticed that the assumed boundary layer thickness is not large enough. However, if we take $y_\infty > 6.6$, then the Newton iteration procedure does not converged. It is observed from Figure 2 that there is because a reversed flow has been detected which causes difficulties in the computation of Equations (25)-(27)

*Orthogonal stagnation-point flow*

The non-dimensional velocity $f'(y)$ and microrotation profiles $h(y)$ for orthogonal stagnation point flow ($\sigma = 0$) are shown in Figure 3 for $\mathrm{Pr} = 1$ and various values of $K$ and $a/c$ when the flow is assisting ($\lambda = 1$) and opposing ($\lambda = -1$). The temperature profiles are similar to those obtained by Ishak *et al.* (2006a) for a Newtonian viscous fluid and therefore they are not presented here. It is seen from Figure 3(a) that all the velocity profiles have the same initial value, namely 1. They have positive slopes for $a/c = 1.5$ (both assisting and opposing flow cases, $\lambda = \pm 1$) and $a/c = 1$ (assisting flow only,$\lambda = 1$). The curves reduce with a negative slope for $a/c = 0.5$ (both assisting and opposing flow cases) and 1 (opposing flow). For the microrotation profiles in Figure 3(b), it is found that, for $a/c = 0.5$, the microrotation reaches a maximum near the wall and then decreases for a further increasing $y$ beyond it. The profiles have the opposite trend for $a/c = 1.5$. Further, it is noticed that the values of $h(y)$ are all positive for $a/c = 0.5$ and they are negative for $a/c = 1.5$. An interesting profile is observed when $a/c = 1.0$, where a reversed flow (change in the direction of rotation) occurs at certain locations of $y$. The value of $h(y)$ changes from negative to positive (for assisting flow), or from positive to negative (for opposing flow), before reaching the value zero. Also, the microrotation increases as $K$ increases.

*Oblique stagnation-point flow*

Tables IV and V show the values of non-dimensional shear stress $\tau_w$ and heat flux from the surface of the sheet $q_w$ for various values of $a/c$, $\sigma$ and $K$ when $\mathrm{Pr} = 1$ and $n = 0$. To illustrate the results obtained, the value of $x$ is taken as unity, and both the assisting and opposing flows ($\lambda = \pm 1$) are considered. It is found that the value of shear stress increases as $K$ increases. On the other hand, the value of heat flux decreases as $K$ increases. It can be seen from both Tables IV and V that for a fixed value of $\sigma$, the shear

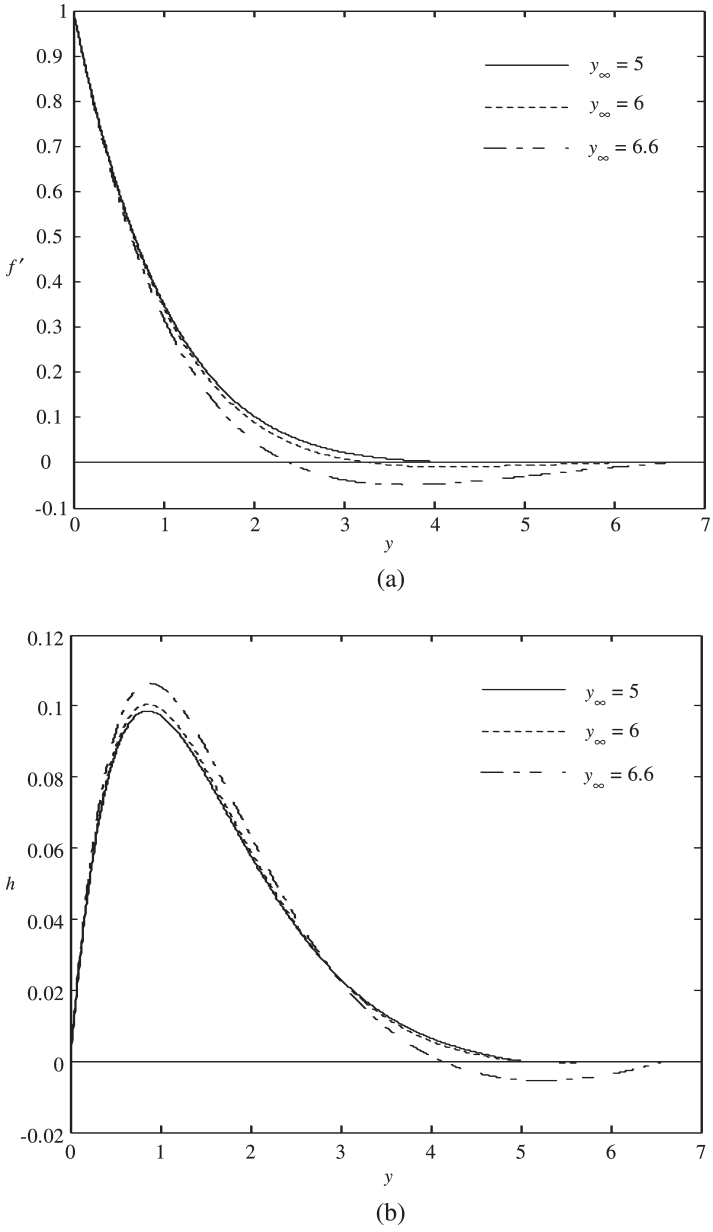


**Figure 2.**
Dimensionless profiles with different boundary layer thickness $y_\infty$ for $\Pr = 1$, $K = 1$, $a/c = 0$ and $\sigma = 0$ (orthogonal stagnation-point flow) when the flow is opposing ($\lambda = -1$); (a) velocity profiles; (b) microrotation profiles

stress and heat flux increase with an increase in $a/c$. For a fixed value of $a/c$, these values increase with an increase in $\sigma$. It is also noticed that the values of shear stress and heat flux for assisting flow are higher than that of opposing flow.

Figure 4 shows the component $U(x, y)$ of the velocity profile as given by Equation (32) for the case of oblique assisting flow ($\lambda = 1$) at a fixed value of $x = 1.0$ and $\sigma = 0.5$ when $n = 0$, $\Pr = 1$ and various values of $a/c$ and $K$. It can be seen clearly that

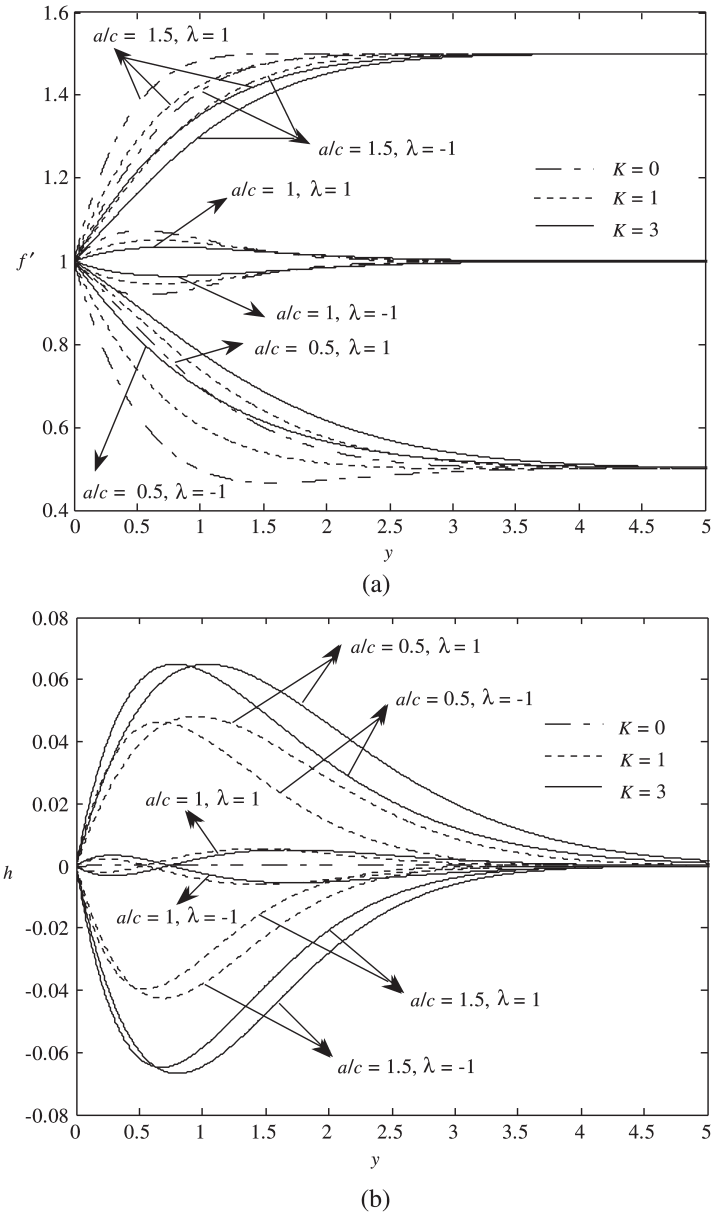


**Figure 3.**
Dimensionless profiles at various values of $a/c$ and $K$ when $\Pr = 1$, $\sigma = 0$ (orthogonal stagnation-point flow) and $\lambda = 1$(assisting flow) or $\lambda = -1$ (opposing flow); (a) velocity profiles; (b) microrotation profiles

the velocity $U$ increases as $a/c$ increases. The flow has a boundary layer structure for values of $a/c > 1$, and the thickness of the boundary layer decreases as $a/c$ increases. The physical explanation for this phenomena has been reported by Mahapatra and Gupta (2002) and Mahapatra *et al.* (2007), where the ratio of the stretching surface $c$ and the shear in the free stream $b$ will affect the straining motion near the stagnation region and this results in the change of boundary layer thickness. It is seen from Figure 4 that

the inverted boundary layer structure exists for values of $a/c < 1$, where the stretching velocity exceeds the stagnation velocity of the external stream. It is also observed that for a fixed value of $y$, the velocity at a point decreases with an increase in the material parameter $K$ for $a/c > 1$, while the velocity increases in $K$ for $a/c < 1$.

| | | Assisting flow ($\lambda = 1$) | | | Opposing flow ($\lambda = -1$) | | |
|---|---|---|---|---|---|---|---|
| $a/c$ | $\sigma$ | $K = 0$ | $K = 1$ | $K = 3$ | $K = 0$ | $K = 1$ | $K = 3$ |
| 0.5 | 0.5 | −0.0033 | 0.0263 | 0.1921 | −0.4959 | −0.5932 | −0.5369 |
| | 1.0 | 0.2779 | 0.5340 | 1.1299 | 0.1019 | 0.1972 | 0.6555 |
| | 1.5 | 0.5592 | 1.0416 | 2.0678 | 0.6997 | 0.9875 | 1.8478 |
| 1.0 | 0.5 | 0.7781 | 1.1614 | 1.8056 | 0.2215 | 0.5136 | 1.0698 |
| | 1.5 | 1.6644 | 2.7063 | 4.5390 | 1.3671 | 2.3454 | 4.1073 |
| 1.5 | 0.5 | 1.7275 | 2.5189 | 3.7038 | 1.1921 | 1.8941 | 2.9916 |
| | 1.0 | 2.2454 | 3.4238 | 5.3017 | 1.7830 | 2.8862 | 4.6891 |
| | 1.5 | 2.7633 | 4.3288 | 6.8995 | 2.3739 | 3.8784 | 6.3866 |

**Table IV.**
Values of $\tau_w = (1 + K)(xF''(0) + G''(0))$ for various values of $a/c$, $\sigma$ and $K$ when $\Pr = 1$, $n = 0$ and $x = 1$

| | | Assisting flow ($\lambda = 1$) | | | Opposing flow ($\lambda = -1$) | | |
|---|---|---|---|---|---|---|---|
| $a/c$ | $\sigma$ | $K = 0$ | $K = 1$ | $K = 3$ | $K = 0$ | $K = 1$ | $K = 3$ |
| 0.5 | 0.5 | 1.2734 | 1.2763 | 1.2810 | 1.2600 | 1.2584 | 1.2671 |
| | 1.0 | 1.3755 | 1.3684 | 1.3643 | 1.4595 | 1.3972 | 1.3734 |
| | 1.5 | 1.4776 | 1.4605 | 1.4477 | 1.6590 | 1.5360 | 1.4798 |
| 1.0 | 0.5 | 1.3683 | 1.3548 | 1.3444 | 1.3313 | 1.3303 | 1.3290 |
| | 1.0 | 1.4540 | 1.4366 | 1.4230 | 1.4426 | 1.4287 | 1.4180 |
| | 1.5 | 1.5397 | 1.5184 | 1.5016 | 1.5538 | 1.5272 | 1.5069 |
| 1.5 | 0.5 | 1.4650 | 1.4347 | 1.4087 | 1.4337 | 1.4135 | 1.3950 |
| | 1.0 | 1.5354 | 1.5043 | 1.4780 | 1.5148 | 1.4909 | 1.4697 |
| | 1.5 | 1.6057 | 1.5739 | 1.5473 | 1.5959 | 1.5683 | 1.5445 |

**Table V.**
Values of $q_w = -(x\theta'(0) + \phi''(0))$ for various values of $a/c$, $\sigma$ and $K$ when $\Pr = 1$, $n = 0$ and $x = 1$

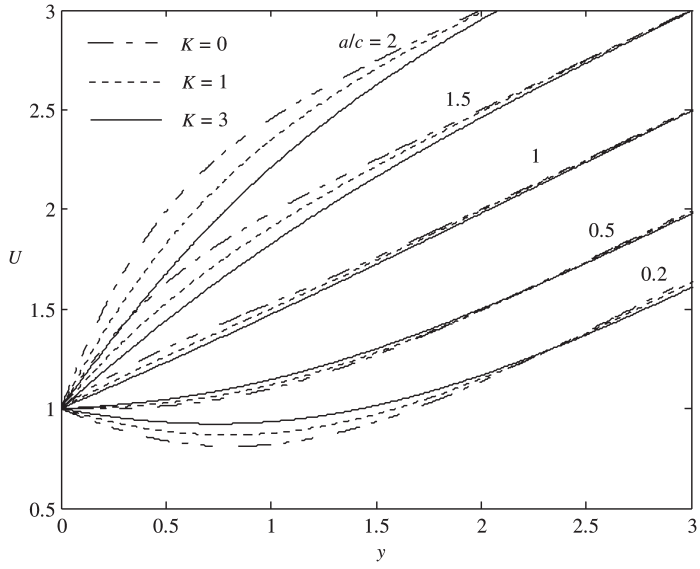


**Figure 4.**
Velocity profiles for various values of $a/c$ and $K$ when $x = \lambda = 1$, $\Pr = 1$, $n = 0$ and $\sigma = 1/2$

Figures 5 and 6 show the microrotation profiles, $N(x, y)$ and temperature profiles, $T(x, y)$ for several values of $a/c$ and $K$ for assisting flow. For $K = 0$, the values of $N(1, y)$ decreases monotonically as $y$ increases, however, for $K = 1$ and 3, the curves reach a minimum point (for $a/c = 2$) or an inflection point appears ($a/c = 0.2$) before they attain the value $N = -0.25$. It should be mentioned here that the value of $N(x, y)$ in the far-flow field of the fluid depends only on the value of the shear flow parameter $\sigma$, see Equation (32). The effect of the parameter $K$ on temperature is opposite to its effect on velocity, where for a fixed value of $y$, the temperature at a point increases with an

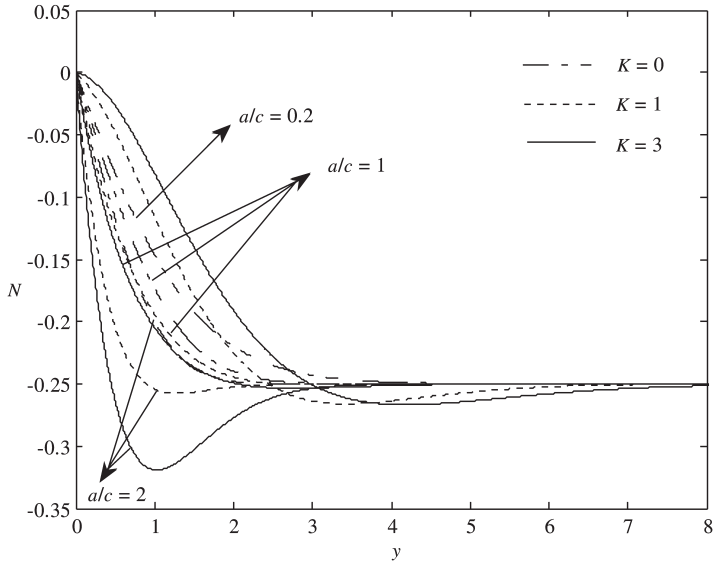


**Figure 5.**
Microrotation profiles for various values of $a/c$ and $K$ when $x = \lambda = 1$, $\Pr = 1$, $n = 0$ and $\sigma = 1/2$

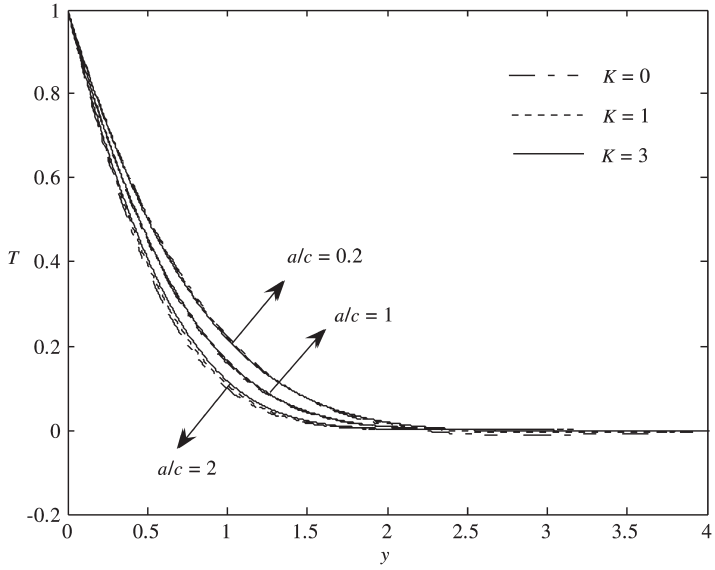


**Figure 6.**
Temperature profiles for various values of $a/c$ and $K$ when $x = \lambda = 1$, $\Pr = 7$, $n = 0$ and $\sigma = 1/2$

increase in the material parameter $K$ for $a/c > 1$, while the temperature decreases in $K$ for $a/c < 1$.

The streamline patterns for the oblique stagnation flows can be obtained from Equation (32). For graphical purposes, we have taken $\Pr = 1$ and $x = 1$. Figure 7 shows the streamline patterns for $a/c = 0.5$, $\sigma = \pm 0.5$, $n = 0$, $K = 0$ and 3 when the flow is assisting. It can be seen that the slope of the dividing streamline far from the plane becomes steeper as $K$ increases. It can be seen that the stagnation point is to

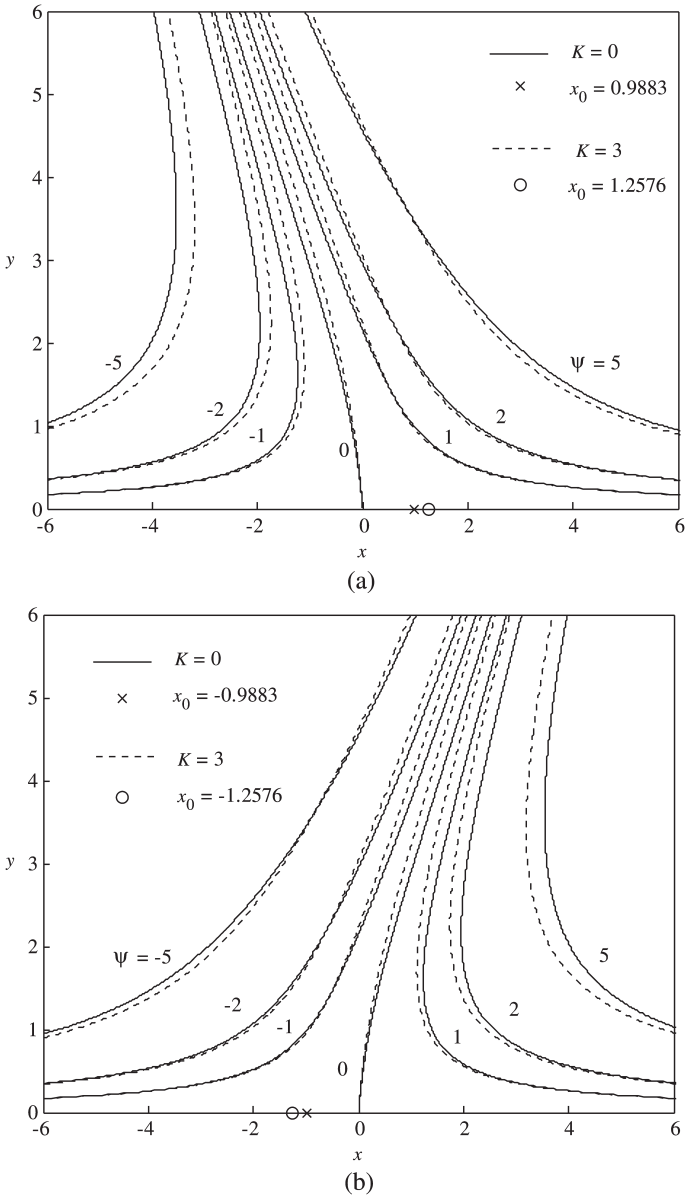


**Figure 7.**
Streamline patterns for $\Pr = 1$, $\lambda = 1$ (assisting flow), $a/c = 0.5$, $n = 0$ (strong concentration) and $K = 0$ and 3; (a) $\sigma = 0.5$; (b) $\sigma = -0.5$

the right of the origin, and its distance from the stagnation-point increases as $K$ increases.

For $a/c = 0.5$, $\sigma = 1$ and $K = 1$, Figure 8(a) shows the comparison of streamlines for micropolar fluid with strong and weak concentration, meanwhile Figure 8(b) shows the comparison between assisting and opposing flows. It is noticed from these figures that the effects of fluid concentration and buoyancy force are not too significant. We observed that the far-flow streamlines are almost parallel to each other and

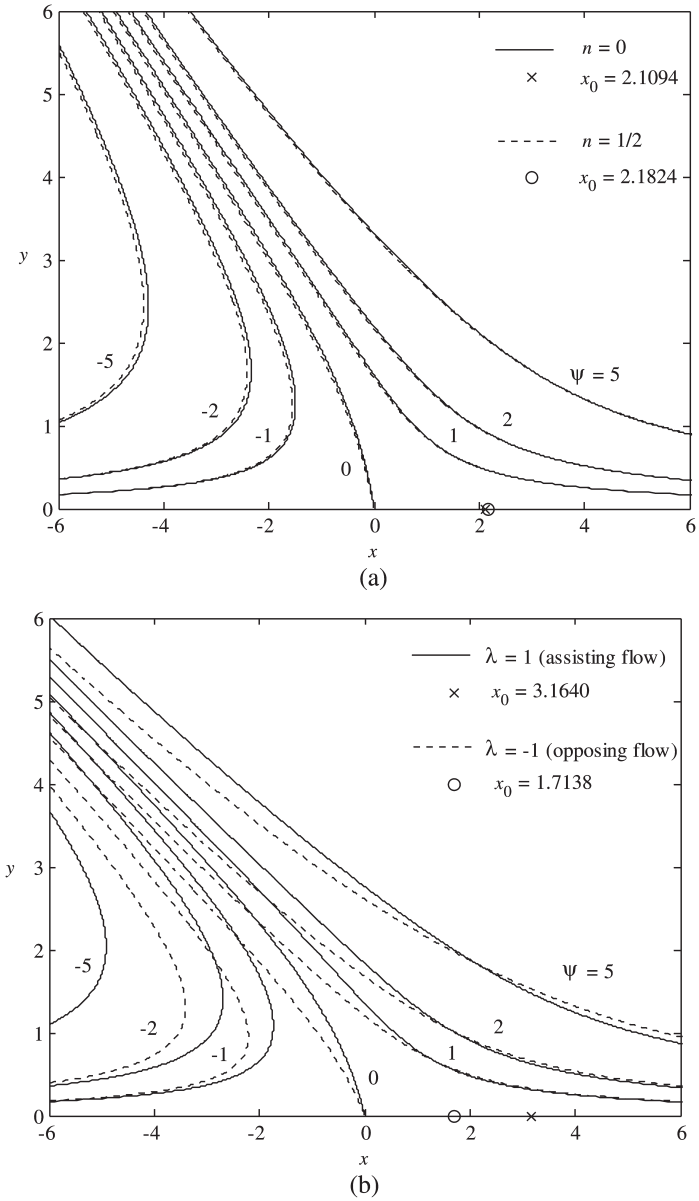


**Figure 8.**
Streamline patterns for Pr = 1, $a/c = 0.5$ and $K = 1$; $\lambda = 1$ (assisting flow), $\sigma = 1$, $n = 0$ (strong concentration) and $n = 1/2$ (weak concentration) (b) $\lambda = 1$ (assisting flow), $\lambda = -1$ (opposing flow), $\sigma = 1.5$ and $n = 0$

asymptotically ended together near the wall surface. However, the locations of the point of zero skin friction for weak concentration and assisting flow are at larger distance from the stagnation-point than they are for strong concentration and opposing flow.

For Figure 8, the streamlines for negative values of $\sigma$ are not shown here because we observed that the streamlines for negative values of $\sigma$ are almost mirror images in the plane $x = 0$ to the streamlines for positive values of $\sigma$. Also, the streamlines become more and more oblique towards the left of the stagnation point with increasing values of $\sigma$ when $b > 0$. On the other hand, the streamlines become increasingly oblique to the right of the stagnation point with an increase in the absolute value of $\sigma$ when $b < 0$. This observation is correct since the shearing motion increases as $\sigma$ increases, which in turn leads to an increase in the obliqueness of the flow towards the stretching sheet, see Mahapatra *et al.* (2007).

Figure 9 presents the streamline patterns for a range of values of $a/c$ for given values of Pr, $\sigma$ and $K$ when the flow is assisting ($\lambda = 1$) and for strong concentration ($n = 0$). It is clear that the obliqueness of the oncoming flow increases as $a/c$ decreases, consequently the shift in the location of zero skin friction. The location zero skin friction is on the right hand side of origin for $a/c < 1$, but this location is on the left hand side of the origin for $a/c \geq 1$.

Table VI shows the values of $R$, i.e. ratio of the slope of the dividing streamline near the wall and far from wall. In order to obtain these values, Equations (33), (35), (37) and (43)-(45) have to be solved along with the boundary conditions (39a) and (46). Various values of $K$ and $a/c$ are considered when $n = 0$ (strong concentration) and $n = 1/2$ (weak concentration) for both assisiting and opposing flows ($\lambda = \pm 1$). It is found that for all the values of Pr, $K$ and $\lambda$ investigated that the values of $R$ decreases with an increase in $a/c$ except in the case of opposing flow, i.e. $\lambda = -1$, where $R$ sometimes decreases then increases and finally decreases again as $a/c$ increases depending on the values of $K$ and $n$. It is also interesting to note that in a number of investigations that the value of $R$ changes sign i.e. the inclination of the dividing streamline at the sheet is

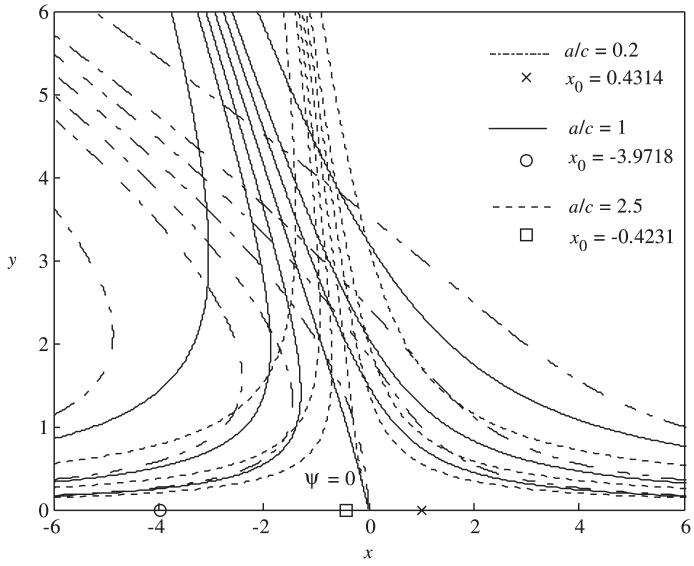


**Figure 9.**
Streamline patterns for various values of $a/c$ when Pr $= 1$, $n = 0$, $K = 1$, $\sigma = 2$ and $\lambda = 1$ (assisting flow)

**Table VI.**
Values of $R$ for various values of $K$ and $a/c$ when Pr = 1, $n$=0 (strong concentration) and $n = 1/2$ (weak concentration) for oblique flow

| | $\lambda = 1$ (assisting flow) | | | | | | $\lambda = -1$ (opposing flow) | | | | | |
|---|---|---|---|---|---|---|---|---|---|---|---|---|
| | $n = 0$ and $1/2$ | $n = 0$ | | $n = 1/2$ | | | $n = 0$ and $1/2$ | $n = 0$ | | $n = 1/2$ | | |
| $a/c$ | $K = 0$ | $K = 1$ | $K = 3$ | $K = 1$ | $K = 3$ | | $K = 0$ | $K = 1$ | $K = 3$ | $K = 1$ | $K = 3$ | |
| 0.1 | −67.6695 | −507.8406 | 161.9614 | −1623.1506 | 84.2997 | | – | 12.9875 | 40.3672 | – | 16.8616 | |
| 0.2 | 43.5251 | 29.3551 | 23.9740 | 22.2588 | 15.2898 | | – | −0.9914 | 13.0032 | −0.6449 | −0.8700 | |
| 0.5 | 3.5556 | 3.9397 | 4.2651 | 3.2244 | 2.9537 | | 1.6727 | 2.5305 | 3.3547 | 1.9139 | 2.1534 | |
| 1.0 | 1.1283 | 1.2946 | 1.4634 | 1.0958 | 1.0658 | | 0.8729 | 1.0918 | 1.3169 | 0.9030 | 0.9326 | |
| 1.5 | 0.6437 | 0.7367 | 0.8345 | 0.6346 | 0.6262 | | 0.5641 | 0.6719 | 0.7855 | 0.5729 | 0.5813 | |
| 2.0 | 0.4464 | 0.5082 | 0.5733 | 0.4426 | 0.4392 | | 0.4118 | 0.4797 | 0.5511 | 0.4154 | 0.4188 | |
| 3.0 | 0.2753 | 0.3108 | 0.3470 | 0.2742 | 0.2732 | | 0.2647 | 0.3018 | 0.3399 | 0.2657 | 0.2667 | |

sometimes positively inclined and sometimes negatively inclined to the dividing streamline at large distances from the sheet. Further, the values of $R$ for micropolar fluids with strong concentration is higher than it is for fluids with weak concentration. Finally, it is noticed that the same difficulties for the orthogonal stagnation-point flow occurs when we perform the calculation for opposing flow with small values of Pr and $a/c$.

## Conclusions

In this paper we have considered the steady two-dimensional stagnation-point flow of an incompressible micropolar fluid which is impinging obliquely on a stretched vertical surface. The stretching velocity and temperature of the surface varies linearly with the distance $x$ from the stagnation point. Both cases of assisting and opposing flows are considered. The transformed ordinary differential equations are solved numerically using the Keller box method for various values of the parameters in $a/c$, $\sigma$, $n$ and $K$. The present results show that for the case of mixed convection flow near an oblique stagnation-point flow, the value of shear stress increases as $K$ increases, while the value of heat flux from the surface of the sheet decreases as $K$ increases. Both the shear stress and heat flux increase with an increase in the parameters $a/c$ and $\sigma$ when $\mathrm{Pr} = 1$. It is also found that the buoyancy force affects the position of the point of zero skin friction, $x_0$.

## References

Ahmadi, G. (1976), "Self-similar solution of incompressible micropolar boundary layer flow over a semi-infinite plate", *International Journal of Engineering Science*, Vol. 14, pp. 639-46.

Ali, M.E. and Al-Yousef, F. (1998), "Laminar mixed convection from a continuously moving vertical surface with suction or injection", *Heat Mass Transfer*, Vol. 33, pp. 301-06.

Ariman, T., Turk, M.A. and Sylvester, N.D. (1973), "Microcontinuum fluid mechanics – a review", *International Journal of Engineering Science*, Vol. 11, pp. 905-30.

Ariman, T., Turk, M.A. and Sylvester, N.D. (1974), "Application of microcontinuum fluid mechanics", *International Journal of Engineering Science*, Vol. 12, pp. 273-93.

Bhargava, R., Kumar, L. and Takhar, H.S. (2003), "Finite element solution of mixed convection micropolar fluid driven by a porous stretching sheet", *International Journal of Engineering Science*, Vol. 41, pp. 2161-178.

Cebeci, T. (2002), *Convective Heat Transfer*, Horizons Publishing, Long Beach, CA.

Cebeci, T. and Bradshaw, P. (1984), *Physical and Computational Aspect of Convective Heat Transfer*, Springer, New York, NY.

Chen, C.-H. (1998), "Laminar mixed convection adjacent to vertical, continuously stretching sheets", *Heat Mass Transfer*, Vol. 33, pp. 471-76.

Chen, C.-H. (2000), "Mixed convection cooling of heated continuously stretching surface", *Heat Mass Transfer*, Vol. 36, pp. 79-86.

Daskalakis, J.E. (1993), "Free convection effects in the boundary layer along a vertically stretching flat surface", *Canadian Journal of Physics*, Vol. 70, pp. 1253-60.

Dorrepaal, J.M. (1986), "An exact solution of the Navier-Stokes equation which describes non-orthogonal stagnation-point flow in two dimensions", *Journal of Fluid Mechanics*, Vol. 163, pp. 141-47.

Dorrepaal, J.M., Chandna, O.P. and Labropulu, F. (1992), "The flow of visco-elastic fluid near a point of reattachment", *Journal of Applied Mathematics and Physics (ZAMP)*, Vol. 43, pp. 708-14.

Eringen, A.C. (1966), "Theory of micropolar fluids", *Journal of Applied Mathematics and Mechanics*, Vol. 16, pp. 1-18.

Eringen, A.C. (1972), "Theory of thermomicrofluids", *Journal of Mathematical Analysis and Applications*, Vol. 38, pp. 480-96.

Eringen, A.C. (2001), *Microcontinuum Field Theories. II: Fluent Media*, Springer, New York, NY.

Gorla, R.S.R. (1988), "Combined forced and free convection in micropolar boundary layer flow on a vertical flat plate", *International Journal of Engineering Science*, Vol. 26, pp. 385-91.

Grubka, L.J. and Bobba, K.M. (1985), "Heat transfer characteristics of a continuous stretching surface with variable temperature", *Journal of Heat Transfer*, Vol. 107, pp. 248-50.

Guram, G.S. and Smith, C. (1980), "Stagnation flows of micropolar fluids with strong and weak interactions", *Computational and Applied Mathematics*, Vol. 6, pp. 213-33.

Hiemenz, K. (1911), "Die Grenzschicht an einem in den gleichförmigen Flüssigkeitsstrom eingetauchten geraden Kreiszylinder", *Dingler Polytechnic Journal*, Vol. 326, pp. 321-24.

Hoyt, J.W. and Fabula, A.G. (1964), "The effect of additives on fluid friction", *US Naval Ordinance Test Station Report*.

Ishak, A., Nazar, R. and Pop, I. (2006a), "Unsteady mixed convection boundary layer flow due to a stretching vertical surface", *Arabian Journal for Science and Engineering*, Vol. 31, pp. 165-82.

Ishak, A. Nazar, R. and Pop, I. (2006b), "Mixed convection boundary layers in the stagnation point flow toward a stretching vertical sheet", *Meccanica*, Vol. 41, pp. 509-18.

Jena, S.K. and Mathur, M.N. (1981), "Similarity solutions for laminar free convection flow of a thermomicropolar fluid past a nonisothermal flat plate", *International Journal of Engineering Science*, Vol. 19, pp. 1431-39.

Kline, K.A. (1977), "A spin-vorticity relation for unidirectional plane flows of micropolar fluids", *International Journal of Engineering Science*, Vol. 15, pp. 131-34.

Labropulu F., Dorrepaal, J.M. and Chandna, O.P. (1996), "Oblique flow impinging on a wall with suction or blowing", *Acta Mechanica*, Vol. 115, pp. 15-25.

Lakshmisha, K.N. Venkateswaran, S. and Nath, G. (1988), "Three-dimensional unsteady flow with heat and mass transfer over a continuous stretching surface", *Journal of Heat Transfer*, Vol. 110, pp. 590-95.

Łukaszewicz, G. (1999), *Micropolar Fluids: Theory and Application*, Birkhäuser, Basel.

Magyari, E. and Keller, B. (1999), "Heat and mass transfer in the boundary layers on an exponentially stretching continuous surface", *Journal of Physics D: Applied Physics*, Vol. 32, pp. 577-85.

Mahapatra, T.R. and Gupta, A.S. (2002), "Heat transfer in stagnation-point flow towards a stretching surface", *Heat Mass Transfer*, Vol. 38, pp. 517-21.

Mahapatra, T.R., Dholey, S. and Gupta, A.S. (2007), "Heat transfer in oblique stagnation-point flow of an incompressible viscous fluid towards a stretching surface", *Heat Mass Transfer*, Vol. 43, pp. 767-73.

Nazar R., Amin, N. and Pop, I. (2003), "Mixed convection boundary-layer flow from a horizontal circular cylinder in micropolar fluids: case of constant wall temperature", *Int. J. Numerical Method for Heat and Fluid Flow*, Vol. 13 No. 1, pp. 86-109.

Partha, M.K., Murthy, P.V.S.N. and Rajasekhar, G.P. (2005), "Effect of viscous dissipation on the mixed convection heat transfer from an exponentially stretching surface", *Heat Mass Transfer*, Vol. 41, pp. 360-66.

Peddieson, J. (1972), "An application of the micropolar fluid model to the calculation of turbulent shear flow", *International Journal of Engineering Science*, Vol. 10, pp. 23-32.

Rees, D.A.S. and Bassom, A.P. (1996), "The blasius boundary-layer flow of a micropolar fluid", *International Journal of Engineering Science*, Vol. 34, pp. 113-24.

Rees, D.A.S. and Pop, I. (1998), "Free convection boundary-layer flow of a micropolar fluid from a vertical flat plate", *IMA Journal of Applied Mathematics*, Vol. 61, pp. 170-97.

Sparrow, E.M. and Abraham, J.P. (2005), "Universal solutions for the streamwise variation of the temperature of a moving sheet in the presence of a moving fluid", *Internatioal Journal of Heat Mass Transfer*, Vol. 48, pp. 3047-56.

Stuart, J.T. (1959), "The viscous flow near a stagnation point when the external flow has uniform vorticity", *Journal of Aerospace Science*, Vol. 26, pp. 124-25.

Takemitsu, N. and Matunobu, Y. (1979), "Unsteady stagnation-point flow impinging obliquely on an oscillating flat plate", *Journal of Physical Society of Japan*, Vol. 47, pp. 1347-53.

Tamada, K.J. (1979), "Two-dimensional stagnation point flow impinging obliquely on a plane wall", *Journal of Physical Society of Japan*, Vol. 46, pp. 310-11.

Tilley, B.S. and Weidman, P.D. (1998), "Oblique two-fluid stagnation-point flow", *European Journal of Mechanics B/Fluids*, Vol. 17, pp. 205-17.

Vleggaar, J. (1977), "Laminar boundary-layer behaviour on continuous accelerating surfaces", *Chemical Engineering. Science*, Vol. 32, pp. 1517-25.

Wang, C.Y. (1985), "The unsteady oblique stagnation point", *Physics of Fluids*, Vol. 28, pp. 2046-49.

**Corresponding author**
I. Pop can be contacted at: pop.ioan@yahoo.co.uk